ISSN 1392-1320 MATERIALS SCIENCE (MEDŽIAGOTYRA). Vol. XX, No. X. 2025

Preparation and Characterization of Activated Carbon (AC) Doped Iron Oxide (Fe_2O_3) Nanoparticles

Chu-yang WANG [1], Yong-liang YANG [2] *

[1] *School of Physics and Optoelectronic Engineering, Nanjing University of Information Science and Technology, Nanjing 210044, Jiangsu, China*
[2] *School of Electrical and Optoelectronic Engineering, Anhui University, He-fei 230601, Anhui, China*

http://doi.org/10.5755/j02.ms.39188

Received 31 October 201X; accepted XX December 201X

This study involves the synthesis of activated carbon (AC) doped iron oxide (Fe_2O_3) nanoparticles by a sol-gel technique, followed by calcination at 600 °C. The prepared nanoparticles are characterized to study the microstructure, optical, magnetic and photocatalytic activity using X-ray diffraction, Field emission scanning electron microscopy, UV-Visible spectroscopy, vibration sample magnetometer, and photoreactor. XRD studies confirmed the presence of Fe_2O_3 phase with the mean crystallite size of 18 nm. The optical studies revealed a bandgap of 2.15 eV. The magnetic studies confirmed the ferromagnetic nature of the nanoparticles. Photocatalytic activity of the nanoparticles was studied for MB dye and found the degradation efficiency of 87 % in 2 h.

Keywords: iron oxide, activated carbon, microstructure, optical properties, photocatalytic activity, magnetic property, nanoparticles

1. INTRODUCTION

Due to the huge population, the necessity of clean drinking water and clean environment increases tremendously. Water and soils are experiencing significant contamination as a result of industrial expansion, urbanisation, and population increase. Contaminated water accounts for 70 – 80 % of all diseases. Heavy metals and poisonous dyes are primary contributors to water pollution, posing a global environmental hazard. There is an immediate necessity for economical solutions for water and wastewater treatment that can satisfy worldwide requirements [1 – 3]. Iron oxide nanotechnology has garnered the interest of researchers to address environmental issues. Iron oxide nanoparticles serve as nano adsorbents offering methods for water purification [4 – 6]. Iron oxides are suitable for various applications, including corrosion science, magnetic devices, photocatalysis, and biomedicine. Iron oxides naturally display polymorphism, with magnetite (Fe_3O_4), maghemite (γ-Fe_2O_3), and haematite (α-Fe_2O_3) being the predominant varieties. Iron oxides possess two valence states, Fe^{2+} and Fe^{3+}, exhibiting magnetic properties and serving effectively as adsorbents for water cleanup. The variable oxidation state of iron allows iron oxides to adopt several phases and single crystalline forms, exhibiting significantly diverse chemical and physical properties. Magnetite (Fe_3O_4) is a magnetic substance, recognised for its magnetic capabilities as a recording medium, and has recently acquired prominence in the domain of spintronics. Moreover, iron oxide nanoparticles are significant in biomedicine owing to their magnetic characteristics and non-toxicity. α-Fe_2O_3 has lately garnered significant interest in the domain of energy storage. At ambient temperature, Fe_3O_4 oxidises to γ-Fe_2O_3, which subsequently converts to the most stable form, α-Fe_2O_3, at temperatures over 300 °C [7 – 9]. Iron oxide is highly effective in eliminating different pollutants via adsorption and photodegradation [10, 11]. Iron oxide serves as an effective adsorbent due to its high surface area, superior magnetic characteristics, biocompatibility, and comparatively inexpensive cost [12, 13]. However, iron oxide possesses a drawback: the agglomeration of nanoparticles resulting from their elevated surface to volume ratio and diminished surface energy [14, 15]. Consequently, surface modification is necessary to avoid agglomeration and aggregation, achieved through doping with activated carbon, which enhances their sorption capacity.

The AC is a form of carbon having a high surface area, making it highly effective at adsorbing molecules. This involves incorporating activated carbon into iron oxide nanoparticles. This was done by chemically integrating them. The doping process aims to enhance the properties of the nanoparticles. Activated carbon is known for its excellent adsorption capabilities. Doping activated carbon with iron oxide nanoparticles can improve their ability to adsorb pollutants, making them useful for environmental clean-up and water purification [16]. The combination of activated carbon with iron oxide nanoparticles can enhance catalytic processes. This can be useful in various chemical reactions, including those used in pollution control and energy production. The presence of activated carbon may influence these magnetic properties, potentially leading to new applications. The combination might lead to synergistic effects where the overall performance of the material is greater than the sum of its individual components. This

* Corresponding author: Y. Yang
E-mail: *07000089@wxc.edu.cn*

could improve performance in applications such as sensors, drug delivery systems, and energy storage [17,18].

Dyes are mostly utilised as colouring agents in the textile sector. The textile and dye industries generate detrimental organic waste, exacerbating environmental contamination. This results from the release of untreated effluents from businesses into water sources. Dyes and heavy metals are mostly released into the environment by chemical manufacturing, electroplating, agriculture, effluents and home wastewater. The activated carbon-doped iron oxide nanoparticles signify a prospective study domain with significant implications across diverse domains, including environmental science and medicine [6, 19, 20]. The nanoparticles were employed to investigate the microstructural, optical, magnetic, and photocatalytic properties.

2. EXPERIMENTAL DETAILS

2.1. Preparation of AC doped iron oxide nanoparticles by sol-gel method

4.353 g of iron nitrate and 0.024 g of activated carbon (AC) were dissolved in 20 ml of DI water separately. These solutions were mixed together and 0.01 g of CTAB was added to the solution. 2.1014 g of citric acid was dissolved in 10 ml of DI water and added as drops to the precursor solution. The temperature was ~ 80 – 90 ºC during the synthesis process and annealed at 600 ºC for 2 h using muffle furnace. The diffraction pattern of the prepared sample was acquired using an X-Ray diffractometer (Rigaku, Japan) with CuKα radiation. The morphology, shape and distribution of the crystallites were determined using a Field Emission Scanning Electron Microscope (Carl Zeiss Microscopy Ltd, UK). The optical absorption spectrum of the synthesized sample was recorded using a UV-visible double beam spectrophotometer (UV-1800, Shimadzu). The vibrating sample magnetometer (VSM, Model 7400-Lake Shore) was used to study the magnetic characteristics of the sample at room temperature. A photocatalytic investigation was conducted utilising photoreactor to analyse the degradation efficiency of AC doped Iron oxide nanoparticles with MB dye.

2.2. Photocatalytic studies

The photocatalytic studies were evaluated using the MB dye with AC/Fe_2O_3 catalyst. The catalyst (1 g/l) was dissolved in the MB dye solution of 10 ppm concentration. The solution was kept under darkness for 30 min to attain equilibrium. The visible light source (550 nm and 125 watts) was used to observe the degradation of MB dye solution for 2 h duration. Following exposure to light, a 2 mL solution was taken at every 30 min intervals and centrifuged subsequently. Then, the spectrophotometer was used to analyse the absorption spectra of the solution collected [21, 22].

3. RESULTS AND DISCUSSION

3.1. Microstructural analysis

X-ray diffraction was used to characterize the crystallinity, structure and phase of the nanoparticles. XRD pattern of AC doped iron oxide is shown in Fig. 1. The sample showed well-defined peaks indicating the crystalline nature. The diffraction peaks were observed at 2θ of 24.20 (012), 33.19° (104), 35.70° (110), 40.90 (113), 49.50° (024), 54.10° (116), 57.6 (018), 62.4° (214) and 64.10 (300) respectively [23].

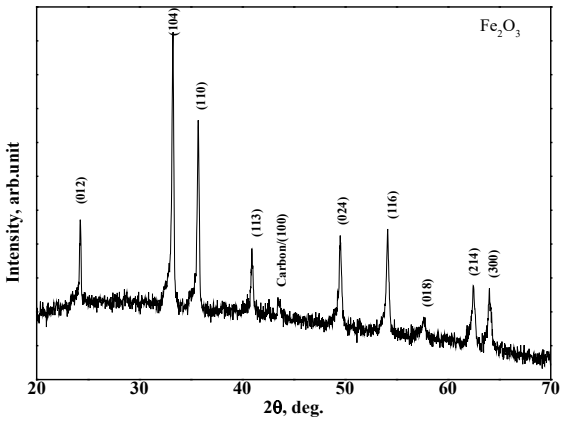

Fig. 1. XRD pattern of the AC doped Fe_2O_3 nanoparticles

The diffracted peaks of the sample coincide well with the standard pattern of the rhombohedral hematite phase. All the peaks correspond to the rhombohedral structure of Fe_2O_3 (JCPDS No. 33-0664). A small peak at 43.5° was detected in the sample, demonstrating the presence of AC within the iron oxide nanoparticles. The crystallite size of the AC-Fe_2O_3 was evaluated by Scherer equation:

$$D = \frac{K\lambda}{\beta \cos\theta}, \quad (1)$$

where λ is the X-ray radiation = 1.5418 Å; b is the full-width at half maximum; θ is the Bragg angle; k is the shape factor (0.9). The crystallite size of the nanoparticles was found to be ~ 8 nm.

Dahlang Tahir et al [24] prepared the Fe_2O_3-carbon composite and the XRD studies confirmed the formation of Fe_2O_3. Settakorn Upasen et al [16] prepared α-Fe_2O_3 NPs using the precipitation method and the TEM analysis showed the hematite nanoparticles with a quasi-spherical shape. Jain et al. [19] synthesised and examined Fe_3O_4 and Fe_3O_4/AC nanoparticles, demonstrating that the iron oxide nanoparticles exhibit a crystalline cubic structure.

The micrographs obtained for the sample are shown in Fig. 2. FE-SEM images provide details about the size, shape, and distribution of the nanoparticles. AC has a tube-like and porous structure with a smooth surface reveal that the nanoparticles are uniform with dense structure. Figure shows the NPs are in uniform size, dense structure with smooth morphology [25].

3.2. Optical properties using UV-visible spectroscopy

The absorbance spectrum was recorded in the 200 – 1000 nm wavelength range (Fig. – 3). The spectrum shows the increase of absorbance, indicating the bandgap of the sample. If the incident energy is equal to the bandgap of the sample, it causes the absorbance to rise. i.e. move from the valence band to the conduction band. The increase of

absorption was found about 600 nm, indicating the shift from VB to CB. The bandgap was obtained using the Tauc plot.

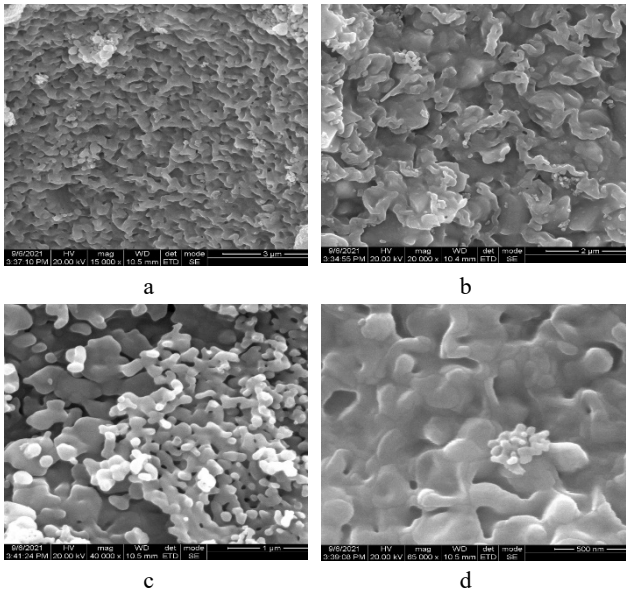

Fig. 2. FESEM images and EDS analysis of the AC doped Fe_2O_3 NPs: a – 15 KX; b – 20 KX; c – 40 KX; d – 65 KX

The equation $(ahv)^2=A\ (hv-E_g)$ was used to find the bandgap of the sample. The energy gap of the sample was evaluated using the Tauc plot, $(ahv)^2$ Vs hv at $\alpha = 0$ (Fig. 3).

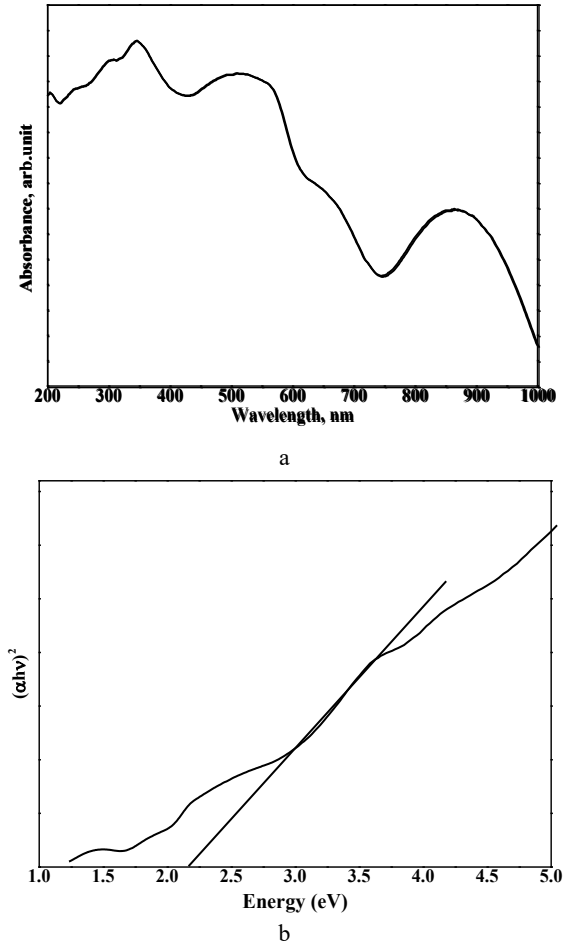

Fig. 3. UV–visible spectroscopy studies of the AC doped Fe_2O_3 sample: a – absorption spectra; b – Tauc plot

Where α is the absorption coefficient, n value is related to the transition type direct or indirect or forbidden. The bandgap of the sample was found to be ~ 2.15 eV, and this value is similar to other reported results. The bandgap of the sample lies between the AC and Fe_2O_3 particles, indicating a good interface between both components, resulting in the bandgap alignment.

The optical absorbance of the iron oxide NPs showed an absorption about 366 nm, indicating the formation of iron oxide [26]. Dahlang Tahir et al. [24] investigated the optical properties. The band gap of Fe_2O_3 is 2 eV, which can be increased by doping with a high bandgap material like activated carbon (AC), (E_g = 4.5 eV), to enhance visible light absorption. The bandgap increased from 2.14 to 2.64 eV with a rise in AC from 10 % to 25 %, respectively. Haghir Ebrahim Abadi and Bagheri-Mohagheghi [25] studied the green synthesized activated carbon /metal oxide properties. The bandgap of nanocomposite showed the two absorption edges, indicating the presence of two materials in the sample, i.e., active carbon and metal oxide. Settakorn Upasen et al. [16] synthesised nanoparticles and found that the sample is considerably higher for light absorption in the visible range.

3.3. Magnetic properties

The magnetization nature of the prepared sample was analysed with vibration sample magnetometer for the applied magnetic field of 0 – 1.5 T range and the observed magnetization nature was shown in Fig. 4. Upon increasing the field from -1.5 T to 1.5 T, the sample's magnetization exhibited a pronounced increase, resulting in an S-shaped curve that produced a hysteresis loop with a coercivity field of around 0.0158 T.

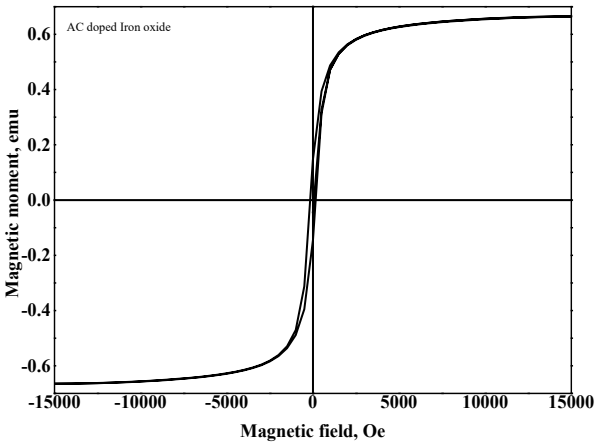

Fig. 4. Magnetisation (M- H) curve of AC doped Fe_2O_3 nanoparticles

The magnetic saturation curves reveal the ferroic nature of the prepared sample and the observed magnetic saturation value of 0.66491 emu of the sample confirms the strong attractive nature as compared to the parent Iron oxide (Fe_2O_3) system [19, 27]. From the magnetization nature, it was noticed that the activated carbon creates a support or matrix that disperses the iron oxide nanoparticles more uniformly. This reduces particle agglomeration (clumping) and allows the individual nanoparticles to maintain their magnetic integrity. Further, the presence of carbon in the nanoparticle matrix can enhance the magnetic anisotropy

property, making it more stable for the magnetic moments to change direction. Henceforth, doping of activated carbon into iron oxide nanoparticles enhances their magnetic stability, saturation magnetization, and coercivity, while also helping to prevent agglomeration and improve dispersibility.

3.4. Photocatalytic properties

Nanoparticles have attracted considerable interest owing to their remarkable properties and several benefits. The adsorption process is a highly effective method for eliminating heavy ions and colours from waste water and has garnered significant interest. Visible light photocatalysis has garnered significant interest owing to its applications in solar energy conversion and environmental remediation under solar illumination. The photocatalytic activity of nanoparticles was examined under visible light conditions (550 nm) for MB dye. The degradation percentage of MB dye was evaluated throughout a reaction duration of 120 min. The degradation of dye relies on both time and concentration. Fig. 5 shows the photocatalytic activity of the sample and illustrates the peak intensity level of the MB dye at its distinctive wavelength in dark conditions. The primary absorption peaks' intensity reduces over time due to the degradation of dyes in the presence of nanoparticles, caused by their absorption in the visible spectrum. Due to its band gap of 2.15 e.V, this material effectively absorbs visible light [11]. The MB photodegradation (%) is determined using the formula [17].

$$\text{MB photodegradation} = (A_0\text{-}A_t)/A_0\times 100, \quad (2)$$

where A_0 and A_t are the initial and final absorbance values of MB, respectively. The AC-Fe_2O_3 NPs showed superior photocatalytic performance, and achieved the degradation efficiency of 87 % within 120 min. The synthesized sample was found to be an excellent photocatalyst under visible light and showed promising results for MB dye degradation.

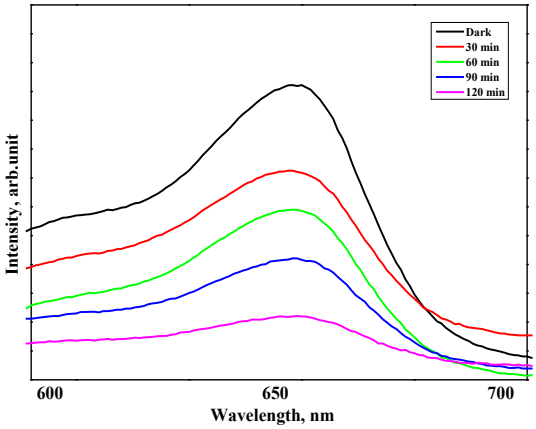

Fig. 5. Photocatalytic degradation of MB dye using AC-Fe_2O_3 catalyst

Upon exposure to visible light, an electron in the photocatalyst is activated, generating electrons and holes. The holes created on the catalyst's surface can react with water to produce hydroxyl radicals, potent oxidants that can oxidise various organic contaminants, leading to their destruction. The photogenerated electron may either recombine with holes or react with available O_2 to generate oxide ions, which might then produce hydroxyl radicals that may further react to form H_2O_2 and further hydroxyl radicals. Dahlang Tahir et al [24] prepared the AC doped Fe_2O_3 nanoparticles and studied the photodegradation using halogen lamp and found the degradation efficiency of 89.51 % in 90 min for 25 % AC. Shabnam Shabanpour and Mehran Riazian [28] prepared the α-Fe_2O_3 nanoparticles and studied the photocatalytic properties for MB dye. The results indicated the breakdown of a complex organic pollutant under UV light, resulting in the total degradation of MB within 90 min. The findings suggest that Fe_2O_3-AC is a viable material for the photodegradation of wastewater through the optimisation of its structural, optical, and magnetic properties.

4. CONCLUSIONS

AC doped α-Fe_2O_3 nanoparticles was synthesized using sol-gel method and calcined at 600 °C for 2 h. XRD studies revealed the formation of α-Fe_2O_3 of rhombohedral structure with the crystallite size of 18 nm. FE-SEM images indicated the formation of nanocrystallites with dense and uniform structure. The Tauc plot derived from the optical absorption spectrum revealed the bandgap of 2.15 eV. The magnetic characteristics revealed the ferroic nature of the AC-Fe_2O_3 nanoparticles. The nanoparticles exhibited higher 87 % degradation efficiency for MB dye under visible light irradiation.

Acknowledgements

This work was supported by West Anhui University high-level talents research start-up fund project (WXRC2023A06).

REFERENCES

1. **Sharififard, H., Nabavinia, M., Soleimani, M.** Evaluation of Adsorption Efficiency of Activated Carbon/Chitosan Composite for Removal of Cr(VI) and Cd(II) from Single and Bi-solute dilute Solution *Advances in Environmental Biology* 4 2016: pp. 215 – 227. https://doi.org/10.22104/aet.2017.484
2. **Pan, T. T., Chen, Z. X., Zhao, H.** Multifunctional catalysts for industrial VOCs oxidation: adaptative active sites and synergistic oxidation effect *Environmental Chemistry and Safety* 1 2025, 9600001. https://doi.org/10.26599/ECS.2025.9600001
3. **Chunmao, C., Hongshuo, C., Xuan, G., Shaohui, G., Guangxu, Y.** Advanced Ozone Treatment of Heavy Oil Refining Wastewater by Activated Carbon Supported Iron Oxide *Journal of Industrial and Engineering Chemistry* 20 2014: pp. 2782 – 2791. https://doi.org/10.1016/j.jiec.2013.11.007
4. **Qu, X., Brame, J., Li, Q., Alvarez, P.J.J.** Nanotechnology for a Safe and Sustainable Water Supply: Enabling Integrated Water Treatment and Reuse *Accounts of Chemical Research* 46 2013: pp. 834 – 843. https://doi.org/10.1021/ar300029v
5. **Zhao, Z., Lan, J., Li, G., Jiang, G.** Iron-based Magnetic Nanomaterials on Wastewater Treatment. In: Reisner, DE, Pradeep T, Editors. Aqua Nanotechnology: Global Prospects. Baton Rouge: CRC Press, 2015: pp. 265 – 91.
6. **Angela, M.G., Thomas, D.D., Zach Hilt, J.** Recent Advances on Iron Oxide Magnetic Nanoparticles as Sorbents

of Organic Pollutants in Water and Wastewater Treatment *Reviews on Environmental Health* 32 2017: pp. 111 – 117. https://doi.org/10.1515/reveh-2016-0063

7. **Huang, Y., Keller. A.A.** Magnetic Nanoparticle Adsorbents for Emerging Organic Contaminants *ACS Sustainable Chemistry & Engineering* 1 (7) 2013: pp. 731 – 736. https://doi.org/10.1021/sc400047q
8. **Samuel, C.N.T., Irene, M.C.L.** Magnetic Nanoparticles: Essential Factors for Sustainable Environmental Applications *Water Research* 47 2013: pp. 2613 – 2632. https://doi.org/10.1016/j.watres.2013.02.039
9. **Xu, J.S., Zhu, Y.J.** γ-Fe_2O_3 and Fe_3O_4 Magnetic Hierarchically Nanostructured Hollow Microspheres: Preparation, Formation Mechanism, Magnetic Property, and Application in Water Treatment *Journal of Colloid and Interface Science* 385 2012: pp. 58 – 65. https://doi.org/10.1016/j.jcis.2012.06.082
10. **Zhang, H.L., Li, X.C., He, G.H., Zhan, J.J., Liu, D.** Preparation of Magnetic Composite Hollow Microsphere and its Adsorption Capacity for Basic dyes *Industrial & Engineering Chemistry Research* 52 2013: pp. 16902 – 16910. https://doi.org/10.1021/ie402404z
11. **Dai Lam, T., Van Hong, L., Hoai, L.P., Thi My, N.H., Thi Quy, N., Thien, T.L., Phuong, T.H., Xuan, P.N.** Biomedical and Environmental Applications of Magnetic Nanoparticles *Advances in Natural Sciences: Nanoscience and Nanotechnology* 1 2010: pp. 045013. https://doi.org/10.1088/2043-6262/1/4/045013
12. **Ilankoon, N.** Use of Iron Oxide Magnetic Nanosorbents for Cr(VI) Removal From Aqueous Solutions: A Review *International Journal* of *Engineering Research and Applications* 4 2014: pp. 55 – 63.
13. **Dave, P.N., Chopda, L.V**. Application of Iron Oxide Nanomaterials for the Removal of Heavy Metals *Journal of Nanotechnololgy* 14 2014: pp. 398569. https://doi.org/10.1155/2014/398569
14. **Ghasemi, N., Ghasemi, M., Moazeni, S., Ghasemi, P., Alharbi, N.S., Gupta, V.K., Agarwal, S.B., Tkachev, A.G.** Zn(II) Removal by Amino-Functionalized Magnetic Nanoparticles: Kinetics, Isotherm, and Thermodynamic Aspects of Adsorption *Journal of Industrial and Engineering Chemistry* 62 2018: pp. 302 – 310. https://doi.org/10.1016/j.jiec.2018.01.008
15. **Ojemaye, M.O., Okoh, O.O., Okoh, A.I.** Surface Modified Magnetic Nanoparticles as Efficient Adsorbents for Heavy Metal Removal from Wastewater: Progress and Prospects *Materials Express* 7 2017: pp. 439 – 456. https://doi.org/10.1166/mex.2017.1401
16. **Settakorn, U.** Activated Carbon-Doped with Iron Oxide Nanoparticles (Fe_2O_3 NPs) Preparation: Particle Size, Shape, and Impurity *International journal of Chem Tech Research* 11 2018: pp. 33 – 40. https://doi.org/10.20902/IJCTR.2018.111006
17. **Oliveira, L.C.A., Rios, R.V.R.A., Fabris, J.D., Garg, S., Lago, R.M.** Activated Carbon/ Iron oxide Magnetic Composites for the Adsorption of Contaminants in Water *Carbon* 40 2002: pp. 2177 – 2183. https://doi.org/10.1016/S0008-6223(02)00076-3
18. **Ruthven, D.M.** Principles of Adsorption and Adsorption Processes, Wiley, New York, 1984.
19. **Monika, J., Mithilesh, Y., Tomas, K., Manu, L., Vinod Kumar, G., Mika, S.** Development of Iron Oxide/Activated Carbon Nanoparticle Composite for the Removal of Cr(VI), Cu(II) and Cd(II) Ions from Aqueous Solution *Water Resources and Industry* 20 2018: pp. 54 – 74. https://doi.org/10.1016/j.wri.2018.10.001
20. **Nikita, G., Susmita, D., Goutam, B., Prabir Kumar, H.** Review on Some Metal Oxide Nanoparticles as Effective Adsorbent in Wastewater Treatment *Water Science & Technology* 85 2022: pp. 3370. https://doi.org/10.2166/wst.2022.153
21. **Yixuan, W., Balakrishnan, G.** Microstructural, Antifungal and Photocatalytic Activity of NiO-ZnO Nanocomposite *Materials Science-Poland* 42 2024: pp. 107 – 115. https://doi.org/10.2478/msp-2024-0006
22. **Liangdong, S., Zhifei, Y., Guojun, S., Zheng, G., Peiyao, L., Balakrishnan, G.** Microstructure and Visible Light Photocatalytic Studies of CeO_2 doped ZnO Nanoparticles. Accepted *Materials Science. (Medziagotyra*) 31 (1) 2025: pp. 22-28. https://doi.org/10.5755/j02.ms.38408
23. **Mohan, N.S., Gokulkumar, R., Shankar, J., Sridharan, R., Logesh, B., Sasikumar, R., Vallarasu, K., Vijayalakshmi, V.** A Facile Green Approach of Fe_2O_3, Fe_2O_3 @Ag, Fe_2O_3 @AC and Fe_2O_3 @Ag@AC NPs Synthesized via Cocos nucifera L for Waste Water Treatment Applications *Results in Chemistry* 4 2022: pp. 100626. https://doi.org/10.1016/j.rechem.2022.100626
24. **Dahlang, T., Sultan, I., Roni, R., Heryanto, H., Ahmad Nurul, F., Mufti Hatur, R., Bualkar, A., Chol Chae, H., Hee Jae, K.** Enhanced Visible-Light Absorption of Fe_2O_3 Covered by Activated Carbon for Multifunctional Purposes: Tuning the Structural, Electronic, Optical, and Magnetic Properties *ACS Omega* 6 2021: pp. 28334 – 28346. https://doi.org/10.1021/acsomega.1c04526
25. **Haghir, E.A.A., Bagheri-Mohagheghi, M.M.** Study of Structure, Morphology, Optical Absorption, and Gap Modulation of Activated Carbon (AC)/NiO, Fe_3O_4, and Co_3O_4 oxide Nanocomposites *Progress in Physics of Applied Materials* 3 2023: pp. 15 – 28. https://doi.org/10.22075/ppam.2023.30469.1054
26. **Suriyaprabha, R., Shivraj Gangadhar, W., Amel, G., Virendra Kumar, Y., Inas, A.A., Jari, S.A., Shakti Devi, K., Timsi, M., Amnah Mohammed, A., Krishna Kumar, Y., Simona, C.** Nanostructured Iron Oxides: Structural, Optical, Magnetic, and Adsorption Characteristics for Cleaning Industrial Effluents *Crystals* 13 2023: pp. 472-485. https://doi.org/10.3390/cryst13030472
27. **Mufti, N., Sari, D.R.P., Muyasaroh, A.F., Yudyanto, Sunaryono, Taufiq, A**. Analyses of Magnetic Properties and Crystal Size on Fe_3O_4 Nanoparticle from Local Iron Sand Using PEG as Soft Template *Journal of Physics: Conference Series* 1595 2020: pp. 012004. https://doi.org/10.1088/1742-6596/1595/1/012004
28. **Shabnam, S., Mehran, R.** Synthesis and Photocatalytic Properties of Nano Iron Oxide *Micro & Nano Letters* 13 2018: pp. 378 – 382. https://doi.org/10.1049/mnl.2017.0635